

Normative Measurements and Apparent Diffusion Coefficient Values of Parotid Lymph Nodes on Magnetic Resonance Imaging

Hatice Kaplanoglu¹, Tuba Akdag¹, Veysel Kaplanoglu² and Aynur Turan¹

¹Department of Radiology, Health Sciences University, Diskapi Yildirim Beyazit Training and Research Hospital, Ankara, Turkey

²Department of Radiology, Health Sciences University, Kecioren Training and Research Hospital, Ankara, Turkey

ABSTRACT

Objective: To determine the morphological features and apparent diffusion coefficient (ADC) values of normal intraparotid lymph nodes (IPLNs) obtained from the MRI examination.

Study Design: Cross-sectional descriptive study.

Place and Duration of Study: Health Sciences University, Diskapi Yildirim Beyazit Training and Research Hospital, Department of Radiology, Ankara, Turkey, from January 2018 to December 2021.

Methodology: The study included 232 patients who underwent neck MRI examination. The long axis diameter (LAD) was measured as the largest diameter of the IPLN, and the short axis diameter (SAD) was measured perpendicular to the LAD. ADC measurements were undertaken by placing the largest region of interest suitable for the size of the IPLNs.

Results: A total of 394 lymph nodes were evaluated. The median LAD and SAD of the lymph nodes were 5.50 (2.50) mm and 3.50 (2.00) mm, respectively. The LAD was 9 mm or lower in 95.7% of the lymph nodes; the SAD was 6 mm or lower in 94.7%. The ADC map was evaluated in 275 IPLNs, with the median ADC value being calculated as $0.77(0.18) \times 10^{-3} \text{ mm}^2/\text{s}$. The ADC value was $1.05 \times 10^{-3} \text{ mm}^2/\text{s}$ or lower in 96.3% of the lymph nodes.

Conclusion: A SAD of 6 mm; and a LAD of 9 mm could be used as normalcy criteria in IPLNs. Normal IPLNs may have an ADC of $1.05 \times 10^{-3} \text{ mm}^2/\text{s}$ or lower. Considering that benign IPLNs may have low ADC values, those can prevent false-positive results in terms of malignancy.

Key Words: Parotid glands, Lymph nodes, Magnetic resonance imaging, Apparent diffusion coefficient.

How to cite this article: Kaplanoglu H, Akdag T, Kaplanoglu V, Turan A. Normative Measurements and Apparent Diffusion Coefficient Values of Parotid Lymph Nodes on Magnetic Resonance Imaging. *J Coll Physicians Surg Pak* 2022; **32(04)**:435-439.

INTRODUCTION

Intraparotid lymph nodes (IPLNs) are one of the critical metastasis sites of head and neck cancers.¹⁻⁵ In addition, head and neck cancer metastasis to the parotid lymph node is generally an unfavourable prognostic factor.⁶ Therefore, it is crucial to identify parotid lymph node metastasis through imaging studies.⁷

Normal values of lymph node sizes differ according to their location. A short-axis diameter (SAD) ≥ 10 mm, a short-long axis diameter ratio of >0.5 , and the presence of necrosis are criteria indicating metastasis in cervical lymph nodes.⁸

Although the characteristics of normal IPLNs were evaluated by ultrasonography and computed tomography (CT) in previous studies,⁹⁻¹¹ to the best of the authors' knowledge, there is only one such study conducted with magnetic resonance imaging (MRI).¹²

To diagnose malignant lymph nodes, morphological features such as size, shape, vascularity, extracapsular spread, calcification, and presence of necrosis, are used. However, these parameters are not sufficient to distinguish between benign and malignant lymph nodes.¹³ Diffusion-weighted (DWI) MRI is superior in detecting lymph node metastasis.¹⁴ DWI is a non-invasive functional technique that examines the microstructure of tissue and lesion. DWI and apparent diffusion coefficient (ADC) maps are based on the analysis of water molecule motion. As the architecture of tissue changes, its ADC value and signal intensity in DWI and ADC maps also change.¹⁵

This study aimed to reveal the normal morphological features and ADC values of IPLNs through the MRI examination.

METHODOLOGY

This study was designed according to the ethical standards of

Correspondence to: Dr. Hatice Kaplanoglu, Department of Radiology, Health Sciences University, Diskapi Yildirim Beyazit Training and Research Hospital, Ankara, Turkey
E-mail: hatice.altknaynak@yahoo.com.tr

Received: November 01, 2021; Revised: December 24, 2021;

Accepted: January 10, 2022

DOI: <https://doi.org/10.29271/jcpsp.2022.04.435>

the Institutional Review Board. Syngo Via console software version 2.0 (Siemens Medical Solutions, Erlangen, Germany) was used to retrospectively examine standard contrast-enhanced neck MRI images in a randomised manner. A total of 500 healthy patients, who underwent a neck MRI examination for any reason between January 2018 and December 2021, were initially included in the study. Patients younger than 18 years and those with a history of trauma, rheumatological disease, or benign or malignant tumoral lesion, were excluded from the study. In addition, patients with a focus of infection for the head and neck region and those with no lymph nodes in the parotid (125 patients), were also excluded in the evaluation process.

ADC measurements were not performed in lymph nodes with a long axis diameter (LAD) of less than 5 mm since their size would reduce the accuracy of the results. Primary demographic data (age and gender) were recorded.

MRI examinations were performed using a standard neck coil with a 1.5 T MRI system (Magnetom Aera; Siemens Healthcare, Erlangen, Germany). The routine neck MRI protocol included pre-contrast axial and coronal spin-echo (SE) T1, axial and sagittal turbo spin-echo (TSE) T2, axial and coronal short tau inversion recovery (STIR), and post-gadolinium (0.1 mmol/kg) post-contrast axial and coronal SE T1 images. Diffusion-weighted single-shot echo-planar images were obtained in the axial plane. DWI was performed in three planes (X, Y, and Z) using three b values (0, 500, and 1,000 s/mm²). The imaging parameters for DWI were as follows: repetition time = 400-600ms, echo time = 80ms, diffusion time = 4.5 seconds, matrix size = 104x128, FOV: 260, slice thickness = 3 mm, and number of acquisitions = 2. ADC maps were automatically created using the Syngo Via console version 2.0.

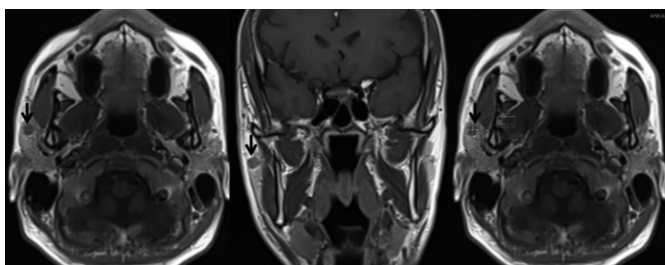


Figure 1: Measurement of the long and short axis diameters of the lymph node (black arrow) in the parotid gland on axial and coronal T1-weighted MRI.

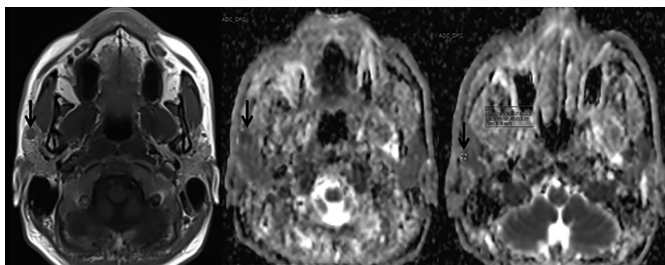


Figure 2: Measurement of the ADC value of the lymph node in the parotid gland in axial T1-weighted MRI by placing a region of interest on the ADC map.

A single radiologist with more than ten years of experience undertook both left and right parotid gland evaluations. Size measurements were performed from the largest IPLN on T1-weighted examinations in the axial plane without fat suppression. The LAD was defined as the largest diameter of the IPLN in the axial plane.¹⁶ The SAD was measured perpendicular to the longest axial diameter (Figure 1).¹⁶ ADC values were measured by placing the largest region of interest suitable for the size of the lymph node on the ADC map (Figure 2).

Mean, standard deviation, for parametric variables median, minimum and maximum values were given in descriptive statistics for non-parametric data, and number and percentage values were given for categorical data. The Shapiro-Wilk test was used to examine the conformity of data to the normal distribution. Stem-and-leaf plot graphics reviewed. In the comparison of the right and left long axis diameter, short axis diameter and ADC values of the patients were analysed by paired samples t-test. Mann-Whitney U-test was used to compare the long and short diameter, ADC values of women and men, and to compare the long and short diameter, ADC values of patients under 50 years of age and over 50 years of age. Wilcoxon test was used to compare the right and left diameter and ADC values of the patients.

IBM SPSS statistics version 20 was used in statistical analyses, and $p < 0.05$ was accepted as the statistical significance limit.

RESULTS

A total of 500 neck MRI images were evaluated, but 268 patients were excluded from the study due to the absence of lymph nodes in the parotid glands in 25% (125), lymph node size being less than 5 mm in 4.8%, benign lesions in the neck in 10.4%, and malignant lesions in the neck in 13.4%. As a result, 232 (46.4%) patients were included in the sample. The mean age of the patients included in the study was 49.90 ± 15.74 years; whereas, 114 (49.1%) were females, and 118 (50.9%) were males. Of all the patients, 69% (160) had lymph nodes in both parotid glands. Thus, a total of 394 IPLNs were evaluated in 232 patients.

Among all the measured IPLNs, the median LAD and SAD were 5.50 (2.50) mm and 3.50 (2.00) mm, respectively (Table I). The LAD was 5 mm or lower in 27.7% (109/394) of the lymph nodes. Due to low reliability, ADC measurement was not performed in lymph nodes with a LAD of less than 5 mm. For the 275 lymph nodes with a LAD of ≥ 5 mm, the median ADC value was $0.77 (0.181) \times 10^{-3} \text{mm}^2/\text{s}$ (Table II). The LAD was 9 mm or lower in 95.7% (377) of the lymph nodes, and the SAD was 6 mm or lower in 94.7% (373). The ADC value was $1.05 \times 10^{-3} \text{mm}^2/\text{s}$ or lower in 96.3% (309/321) of the lymph nodes. There was no significant difference in the LAD and SAD, and the ADC values between the male and female patients ($p = 0.400$).

For the 193 (49%) patients with lymph nodes in the right parotid, the median LAD was 5.10 (3.00) mm, and the median SAD was 3.20 (1.50) mm.

Table I: Comparison of the long and short axis diameters.

	n (%)	Long axis diameter (mm)		Short axis diameter (mm)	
		Median (IQR)	p-value	Median (IQR)	p-value
Overall	394 (100)	5.50 (2.50)		3.50 (2.00)	
Female	189 (48)	5.50 (2.40)	0.746	3.50 (1.50)	0.432
Male	205 (52)	5.50 (3.00)		3.40 (1.75)	
Right	163 (49)	5.50 (2.50)	0.010	3.50 (1.50)	0.010
Left	163 (49)	6.00 (2.30)		3.50 (2.00)	

*Mann-Whitney U-test was used to compare long axis diameter and short axis diameter values of women and men.
*Wilcoxon test was used to compare the right and left long axis diameter and short axis diameter values of the patients.

Table II: ADC values of lymph nodes with long axis diameter ≥5 mm.

	n (%)	Median (IQR)	p-value
ALN	275 (100)	770.49 (181.63)	
Female	137 (49.8)	783.46 (183.15)	0.400
Male	138 (51.2)	762.87 (176.80)	
<50 years	132 (48)	798.55 (188.75)	0.007
≥50 years	143 (52)	751.95 (185.82)	
Right	109 (39.6)	782.11 (163.85)	0.387
Left	109 (39.6)	768.00 (174.66)	

*Mann Whitney U-test was used to compare the ADC values of women and men.
*The Mann-Whitney U-test was used to compare the ADC values of patients younger than 50 years of age and patients 50 years and older. *Wilcoxon test was used to compare the right and left ADC values of the patients.

Table III: Lymph node measurements and ADC values of the patients.

	Median (IQR)
Right lymph node, long axis diameter (n = 193)	5.10 (3.00)
Right lymph node, short axis diameter (n = 193)	3.20 (1.50)
Right ADC (n = 156)	774.26 (179.90)
Left lymph node, long axis diameter (n = 201)	6.00 (2.50)
Left lymph node, short axis diameter (n = 201)	3.50 (2.00)
	Mean ± SD
Left ADC (n = 165)	780.45 ± 152.13

ADC: Apparent diffusion coefficient.

Among the 201(51%) patients with lymph nodes in the left parotid, the median LAD and SAD were determined as 6.00 (2.50) and 3.50 (2.00) mm, respectively. Both LAD and SAD were larger in the left parotid lymph nodes compared to the right side (p = 0.010 and p = 0.010, respectively). The median ADC values of the lymph nodes were 0.774 (0.179) x10⁻³mm²/s on the right side and 0.766 (0.290) x10⁻³mm²/s on the left side (Table III). There was no significant difference between the ADC values of the right and left parotid lymph nodes (p=0.387, Table II).

DISCUSSION

Due to the late formation of the capsule structure during embryological development, the parotid glands have their internal lymph nodes, unlike other salivary glands. Cadaver studies have revealed the presence of IPLN in normal parotid glands in 90% of the cases.¹⁷ Parotid lymph nodes receive lymphatic drainage primarily from the scalp and skin around the eyes, as well as from the nasopharynx. IPLNs are an important site of head and neck cancer metastasis, most commonly squamous cell carcinoma and melanoma, and

less frequently oral cavity cancer. It has been reported that independent of lymph node metastasis in the neck, IPLN metastasis is a poor prognostic factor for the malignant tumors of the parotid gland itself, primary head and neck squamous cell carcinoma, and malignant melanoma.¹⁸

An accurate evaluation of IPLNs is essential in the staging and treatment decisions in head and neck cancers. The clinical assessment of IPLNs by palpation is complex; therefore, radiological imaging methods are crucial in the diagnosis. While these evaluations can be performed primarily with ultrasonography, CT, and MRI, a fine-needle aspiration biopsy may be required for further examination. In the current study, MRI was chosen considering its increasing use in evaluating head and neck cancers. In addition, MRI may evaluate the extent of local disease better than CT; and the DWI sequence can be used to reveal tumor burden.¹⁹ MRI is also superior to CT in the evaluation of small lymph nodes.¹⁹

Studies on IPLNs, using cross-sectional imaging methods, are limited. In a CT-based study, Zhang *et al.* reported that the LAD was 7 mm or lower in 96% of benign IPLNs, and the SAD was 7 mm or lower in 93%.⁸ In this study, 95.7% of the IPLNs had ≤9 mm LAD, and 94.7% of the IPLNs had ≤6 mm SAD. As a result of their CT measurements, Zhang *et al.* recommended the normal upper limit of the SAD of benign IPLNs as 5 mm.⁸ In this study, in the evaluation of benign IPLNs, the authors found the upper limit of the SAD to be 6 mm on MRI. In addition, in contrast to Zhang *et al.*, it is observed that the benign lymph nodes in the left parotid gland had significantly larger SAD and LAD when compared to those located on the right.

In addition to determining the size and morphology of IPLNs in MRI, DWI may also provide a functional perspective with imaging. Today, DWI is almost always used in neck MRI examinations because it is non-invasive, can be applied easily in a short time, and allows for quantitative measurements. The current literature supports the idea that different values obtained by calculating the ADC values of tissues and lesions can be used to differentiate benign and malignant cases.²⁰ Thus, DWI is gaining increasing importance in head and neck imaging. The main indications for DWI in this relatively small but challenging area of the body are tissue characterisation, nodal staging, and early detection of treatment failure by distinguishing post-treatment recurrent or residual tumors from postoperative changes. In patients responding well to

treatment, there is an increase in the ADC values in primary tumors and nodal metastases, while the ADC value does not change or even tend to decrease in unresponsive lesions during follow-up.²¹ Compared with the ADCs of benign lesions, lower ADC values have been reported for most malignant lesions.²¹ For nodal staging, DWI has been reported to be promising to help detect lymph node metastases based on low ADC values even in small lymph nodes, compared to normal or reactive lymph nodes.²¹

Chen *et al.* defined $1.01 \times 10^{-3} \text{ mm}^2/\text{s}$ as an optimal cut-off value in distinguishing benign and malignant IPLNs.¹² This is interpreted as IPLNs with an ADC value below $1.01 \times 10^{-3} \text{ mm}^2/\text{s}$ being more likely to be malignant. In this study, the ADC value was $1.05 \times 10^{-3} \text{ mm}^2/\text{s}$ or lower in 96.3% of the benign IPLNs. In other words, unlike Chen *et al.*, this study showed that IPLNs with a mean ADC value of fewer than $1.01 \times 10^{-3} \text{ mm}^2/\text{s}$ could also be benign and that benign lymph nodes might have a broader range of ADC values. The authors consider that accepting values of $1.01 \times 10^{-3} \text{ mm}^2/\text{s}$ and below, as a malignancy criterion for IPLNs, may lead to an unfounded suspicion of malignancy in patients; and may result in unnecessary biopsy procedures. DWI is still a new and unoptimised technique. The successful application of this technique will be achieved over time through the optimisation and standardisation of parameters in DWI, comparison of images with morphological images, and growing experience. It is essential to conduct further studies on small metastases and complex anatomical regions, such as the head and neck.

Although it was intended to perform a detailed morphological and functional evaluation of benign IPLNs in this study, there were certain limitations. Despite the strict exclusion criteria, the first and most important limitation was the absence of a pathological diagnosis in any lymph node. Although it is not possible to use an invasive method to prevent such a limitation, the sample containing no patient with any known malignancy, rheumatological disease, the focus of infection, or trauma history was the most vital aspect of the study in describing IPLNs as benign. Another limitation to be considered is the absence of inter-observer and intra-observer variability in the measurements of the lymph nodes.

CONCLUSION

A SAD of 6 mm and a LAD of 9 mm could be used as benignity criteria in IPLNs, and benign IPLNs could have an ADC of $1.05 \times 10^{-3} \text{ mm}^2/\text{s}$ or lower. Therefore, the authors consider that low ADC values as a malignancy criterion can lead to false-positive results.

ETHICAL APPROVAL:

The study was approved by the Clinical Trials Ethics Committee before the initiation of the study (Approval No. 09.08.2021/ 117/03).

PATIENTS' CONSENT:

All participants provided informed consent before taking part in the study.

CONFLICT OF INTEREST:

The authors declared no conflict of interest.

AUTHORS' CONTRIBUTION:

HK: Design of the work; acquisition, analysis and interpretation of data; drafting the article; revising it critically for important intellectual content the article.

TK: Drafting the article; revising it critically for important intellectual content.

VK: Acquisition, analysis and interpretation of data.

AT: Revising it critically for important intellectual content.

All the authors gave final approval of the version to be published.

REFERENCES

1. Harada H, Omura K. Metastasis of oral cancer to the parotid node. *Eur J Surg Oncol* 2009; 35(8):890-4. doi: 10.1016/j.ejso.2008.09.013.
2. Niu X, Fang Q, Liu F. Role of intraparotid node metastasis in mucoepidermoid carcinoma of the parotid gland. *BMC Cancer* 2019; 19(1):417. doi: 10.1186/s12885-019-5637-x.
3. Thom JJ, Moore EJ, Price DL, Kasperbauer JL, Starkman SJ, Olsen KD. The role of total parotidectomy for metastatic cutaneous squamous cell carcinoma and malignant melanoma. *JAMA Otolaryngol Head Neck Surg* 2014; 140(6):548-54. doi: 10.1001/jamaoto.2014.352.
4. Wang HZ, Cao CN, Luo JW, Yi JL, Huang XD, Zhang SP, *et al.* High-risk factors of parotid lymph node metastasis in nasopharyngeal carcinoma: A case-control study. *Radiat Oncol* 2016; 11(1):113. doi: 10.1186/s13014-016-0691-x.
5. Wang S, Lou J, Zhang S, Guo L, Wang K, Ge M. Metastasis of nasopharyngeal carcinoma to parotid lymph nodes: A retrospective study. *World J Surg Oncol* 2015; 13:1. doi: 10.1186/1477-7819-13-1.
6. Ch'ng S, Maitra A, Lea R, Brasch H, Tan ST. Parotid metastasis-an independent prognostic factor for head and neck cutaneous squamous cell carcinoma. *J Plast Reconstr Aesthet Surg* 2006; 59(12):1288-93. doi: 10.1016/j.bjps.2006.03.043.
7. Kashiwagi N, Murakami T, Toguchi M, Nakanishi K, Hidaka S, Fukui H, *et al.* Metastases to the parotid nodes: CT and MR imaging findings. *Dentomaxillofac Radiol* 2016; 45(8):20160201. doi: 10.1259/dmfr.20160201.
8. Lan M, Huang Y, Chen CY, Han F, Wu SX, Tian L, *et al.* Prognostic value of cervical nodal necrosis in nasopharyngeal carcinoma: Analysis of 1800 patients with positive cervical nodal metastasis at MR imaging. *Radiology* 2015; 276(2):536-44. doi: 10.1259/dmfr.20160201.
9. Zhang MH, Ginat DT. Normative measurements of parotid lymph nodes on CT imaging. *Surg Radiol Anat* 2020; 42(9):1109-12. doi: 10.1007/s00276-020-02494-8.
10. Ying M, Ahuja A. Sonography of neck lymph nodes. Part I: Normal lymph nodes. *Clin Radiol* 2003; 58:351-8. doi:

- 10.1007/s00276-020-02494-8.
11. Ying M, Ahuja A, Brook F, Brown B, Metreweli C. Sonographic appearance and distribution of normal cervical lymph nodes in a Chinese population. *J Ultrasound Med* 1996; 15(6):431-6. doi: 10.7863/jum. 1996.15.6.431.
 12. Chen C, Lin Z, Xiao Y, Bai P, Yue Q, Chen Y, et al. Role of diffusion-weighted imaging in the discrimination of benign and metastatic parotid area lymph nodes in patients with nasopharyngeal carcinoma. *Sci Rep* 2018; 8(1):281. doi: 10.7863/jum.1996.15.6.431.
 13. de Bondt RB, Hoeberigs MC, Nelemans PJ, Deserno WM, Peutz-Kootstra C, Kremer B, et al. Diagnostic accuracy and additional value of diffusion-weighted imaging for discrimination of malignant cervical lymph nodes in head and neck squamous cell carcinoma. *Neuroradiol* 2009; 51(3):183-92. doi: 10.1007/s00234-008-0487-2.
 14. Sumi M, Sakihama N, Sumi T, Morikawa M, Uetani M, Kabasawa H, et al. Discrimination of metastatic cervical lymph nodes with diffusion-weighted MR imaging in patients with head and neck cancer. *AJNR Am J Neuroradiol* 2003; 24(8):1627-34. doi: 10.1007/s00234- 008-0487-2.
 15. Schafer J, Srinivasan A, Mukherji S. Diffusion magnetic resonance imaging in the head and neck. *Magnetic Reson Imag Clin* 2011; 19(1):55-67. doi: 10.1016/j.mric. 2010.10.002.
 16. Ganeshalingam S, Koh D-M. Nodal staging. *Cancer Imaging* 2009; 9:104-11. doi: 10.1016/j.mric.2010.10.002.
 17. Sonmez Ergün S, Gayretli O, Büyükpınarbaşı N, Yıldız K, Gürses İA, Avcı A, et al. Determining the number of intraparotid lymph nodes: postmortem examination. *J Cranio-maxillofac Surg* 2014; 42(5):657-60. doi: 10.1016/j.jcms.2013.09.011.
 18. Guntinas-Lichius O, Thielker J, Robbins KT, Olsen KD, Shaha AR, Makitie AA, et al. Prognostic role of intraparotid lymph node metastasis in primary parotid cancer: Systematic review. *Head Neck* 2021; 43(3): 997-1008. doi: 10.1002/hed.26541.
 19. Abdel Razeq AA, Soliman NY, Elkhamary S, Alsharaway MK, Tawfik A. Role of diffusion-weighted MR imaging in cervical lymphadenopathy. *Eur Radiol* 2006; 16(7): 1468-77. doi: 10.1002/hed.26541.
 20. Thoeny HC, De Keyzer F, King AD. Diffusion-weighted MR imaging in the head and neck. *Radiology* 2012; 263(1):19-32. doi: 10.1148/radiol.11101821.
 21. Hermans R. Diffusion-weighted MRI in head and neck cancer. *Curr Opin Otolaryngol Head Neck Surg* 2010; 18(2):72-8. doi: 10.1097/MOO.0b013e32833555f2.

